Taylor & Francis
Taylor & Francis Group

Check for updates

RESEARCH PAPER

Aberrant hydroxymethylation of *ANGPTL4* is associated with selective intrauterine growth restriction in monochorionic twin pregnancies

Yi Zhang [a*], Dezhong Zheng[b,c*], Qun Fang[d], and Mei Zhong[a]

aDepartment of Obstetrics and Gynecology, Nanfang Hospital, Southern Medical University, Guangzhou, China; bDepartment of Cardiology, The Third Affiliated Hospital of Southern Medical University, Southern Medical University, Guangzhou, China; cDepartment of Cardiology, Nanfang Hospital, Southern Medical University, Guangzhou, China; dDepartment of Obstetrics and Gynecology, The First Affiliated Hospital of Sun Yat-sen University, Sun Yat-sen University, Guangzhou, China

ABSTRACT

Selective intrauterine growth restriction (sIUGR) is a severe complication in monochorionic (MC) twin pregnancies, and it carries increased risks of poor prognosis. Current data suggest that vascular anastomoses and unequal placental sharing may be the key contributor to discordant foetal growth. While MC twins derive from a single zygote and have almost identical genetic information, the precise mechanisms remain unknown. DNA hydroxymethylation is a newly discovered epigenetic feature associated with gene regulation and modification. Here, we investigate discordant hydroxymethylation patterns between two placental shares of sIUGR and analyse the potential role of aberrant hydroxymethylation of angiopoietin-like 4 (*ANGPTL4*) in placental dysplasia. Hydroxymethylation DNA immunoprecipitation (hMeDIP)-chip and mRNA sequencing were performed to identify hydroxymethylation-associated genes. Real-time qPCR, western blotting, and immunohistochemistry were used to confirm *ANGPTL4* expression. The mechanisms regulating *ANGPTL4* were investigated by cell migration assay, invasion assay, viability assay, and apoptotic ratio assays, western blotting and hMeDIP-qPCR. Decreased *ANGPTL4* was detected in the smaller placental shares of sIUGR. *ANGPTL4* knockdown suppressed trophoblast invasiveness and migration, which possibly occurred through hypoxia inducible factor 1α (*HIF-1α*) and *HIF-1* signalling pathway. Hypoxia leads to aberrant expression of *ANGPTL4* and *HIF-1α*, positively correlated with their aberrant hydroxymethylation levels in promoter regions. Aberrant hydroxymethylation of *ANGPTL4* may contribute to placental impairment by the *HIF-1* signalling pathway in smaller placental shares of sIUGR.

Introduction

Selective intrauterine growth restriction (sIUGR) affects approximately 10–15% of monochorionic (MC) twin pregnancies, and it is associated with an increased risk of perinatal mortality and morbidity [1]. Although previous studies have reported that the pathogenesis of sIUGR relies on discordant placental sharing and vascular anastomoses, the underlying molecular mechanisms remain obscure [2]. MC twins, which derive from a single zygote, harbour almost identical genetic information and share a similar intrauterine environment, so epigenetic events may be involved in these mechanisms [3].

DNA hydroxymethylation is a stable epigenetic modification that plays unique regulatory roles in various physiopathological processes [4]. 5-Hydroxymethylcytosine (5 hmC, the marker of hydroxymethylation) is distributed in various different tumours or different development stages, suggesting that it may have key roles in different cancers and disorders [5–7]. The distribution of 5 hmC can be found at the enhancer, promoter, transcription start site (TSS), gene body, 3'UTR or intragenic region, so the function and mechanism of 5 hmC need to be further investigated [8].

The placenta is a temporary organ that plays a critical role in sustaining pregnancy and foetal growth. Placental dysplasia is considered to be a central feature of pregnancy-associated disorders

CONTACT Mei Zhong ✉ zhongmei@smu.edu.cn 🖃 Department of Obstetrics and Gynecology, Nanfang Hospital, Southern Medical University, 1838 Guangzhou Avenue North, Guangzhou 510515, China; Qun Fang ✉ fang__qun@163.com 🖃 Department of Obstetrics and Gynecology, The First Affiliated Hospital of Sun Yat-sen University, Sun Yat-sen University, 58 Zhongshan 2nd Road, Guangzhou 510080, China
*These authors contributed equally to this work.

such as preeclampsia (PE) or foetal growth restriction (FGR) [9,10]. Accumulating evidence has shown that epigenetic factors such as microRNAs, imprinted genes or DNA methylation may take part in placental impairment [2,11,12]. In contrast to singleton pregnancy, sIUGR twins are considered an optimal model for exploring epigenetic molecular mechanisms due to the exclusion of effects from different genetic backgrounds among individuals.

Our preliminary data suggested that the level of genome-wide DNA hydroxymethylation was significantly decreased in smaller placental shares compared to the larger ones in sIUGR, as shown by ultra-performance liquid chromatography/tandem mass spectrometry (UPLC-MS/MS) technology [2]. Thus, we hypothesized that discordant DNA hydroxymethylation statuses might be important for placental dysfunction and growth discordance between two foetuses of sIUGR.

Angiopoietin-like 4 (ANGPTL4) is a hypoxia responsive gene regulating vascular permeability, angiogenesis, and inflammation [13]. ANGPTL4 is also a downstream target of hypoxia inducible factor 1α (HIF-1α), and it is regulated by HIF-1α in various cell types [14]. However, few studies have reported the regulatory relationship of DNA hydroxymethylation between HIF-1α and ANGPTL4 in placental insufficiency and foetal growth. In this study, we first identified differential hydroxymethylation patterns between two placental shares of sIUGR and then tried to reveal and validate an epigenetic-mediated mechanism mainly focused on hypoxia-induced aberrant hydroxymethylation of ANGPTL4 and HIF-1α. The results may highlight a potential mechanism between hydroxymethylation modification and discordant foetal growth or even placenta-associated disorders.

Results

Clinical data

Clinical characteristics are summarized in Table 1. Both the smaller and larger foetal weights were significantly lower in the sIUGR group than in the normal group ($p = 0.000 < 0.01$). The intertwin difference in birth weight was significantly larger in the sIUGR group than in the normal group ($p = 0.000 < 0.01$). The gestational age of delivery was much earlier in the sIUGR group than in the normal group ($p = 0.000 < 0.01$). No significant difference was found between the maternal age in the sIUGR and normal groups ($p = 0.995 > 0.05$).

## Distributions of DhMRs and identifying hydroxymethylation-associated genes

Hydroxymethylation DNA immunoprecipitation (hMeDIP)-chip and mRNA sequencing (mRNA-seq) were performed to examine the differential distributions of 5hmC and hydroxymethylation-associated genes between two placental shares in four sIUGR twin pairs and four normal MCDA twin pairs (Figure 1(a,b)). Compared with the normal group, 181 upregulated genes and 614 downregulated genes were identified in smaller placental shares of the sIUGR group (Figure 1(c), supplement figure S1). Furthermore, we subdivided promoter regions into three classes based on the CpG ratio, GC content, and length of the CpG-rich region as previously reported: high CpG-density promoters (HCPs), low CpG-density promoters (LCPs) and intermediate CpG-density promoters (ICPs) [15]. Compared with the normal group, there were 729 differential hydroxymethylation regions (DhMRs) in HCPs, 239 DhMRs in ICPs and 198 DhMRs in LCPs identified in the sIUGR group (supplement Table S1). Combination analysis of Gene Ontology

Table 1. Characteristics of sIUGR and normal MCDA twin pregnancies.

	sIUGR(n = 13)	Normal(n = 18)	*p* value
Maternal age (years)	31.85 ± 5.37	31.83 ± 5.39	0.995
Gestational age (weeks)	32.58 ± 2.19	36.02 ± 1.17	0.000**
Birth weight of larger twin (kg)	1.83 ± 0.34	2.47 ± 0.27	0.000**
Birth weight of smaller twin (kg)	1.22 ± 0.30	2.33 ± 0.30	0.000**
Birth weight discordance (%)	33.74%±8.50%	5.71%±3.68%	0.000**

Data are shown as the mean ± SD. **$p < 0.01$
sIUGR: selective intrauterine growth restriction. Normal: normal MCDA twins.
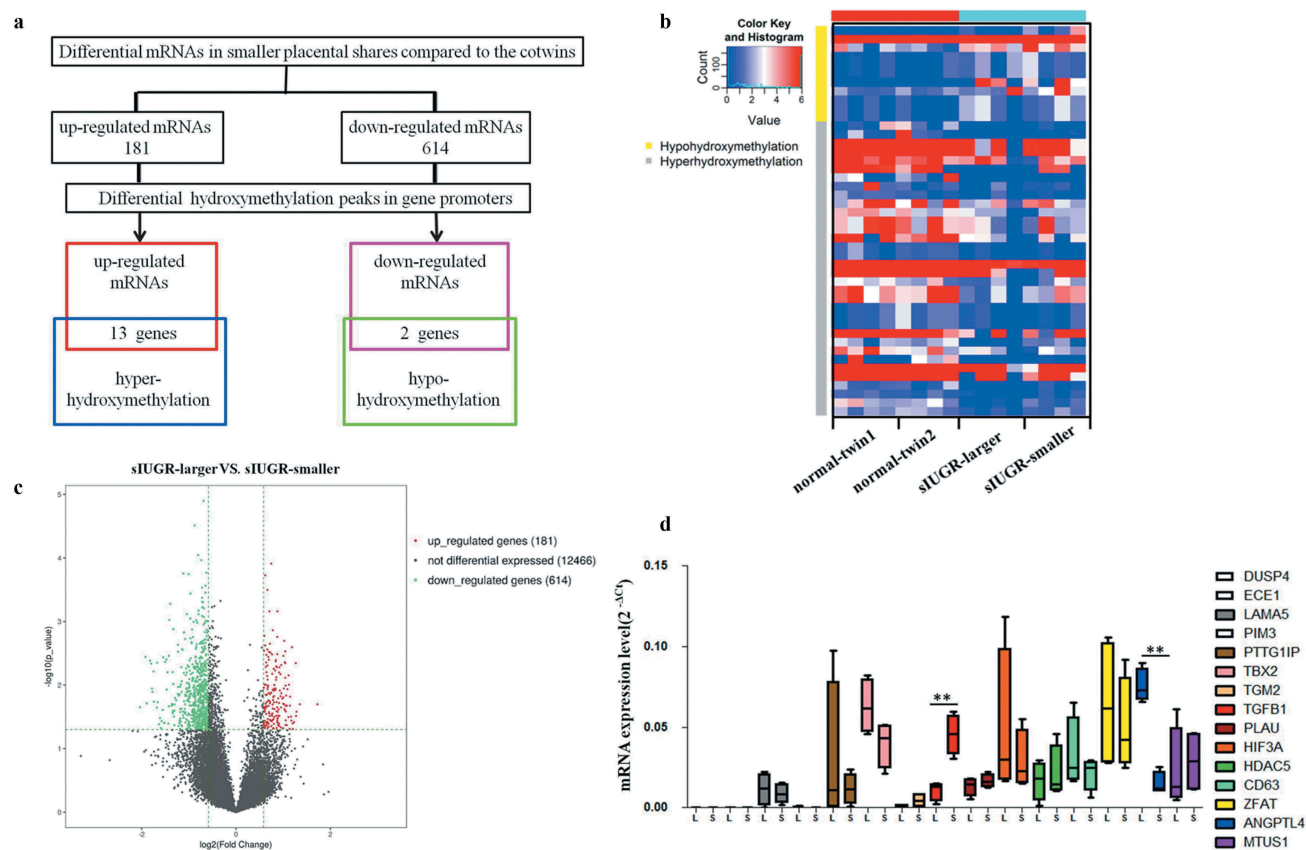
Figure 1. Hydromxymethylation-associated genes detected in sIUGR twin pairs through hMeDIP-chip and mRNA sequencing. (a) Schematic representation for identifying hydroxymethylation-associated genes. The putative targets obtained by overlapping the differentially expressed mRNAs and differentially hydroxymethylation peaks in promoter region. (b) The differentially expressed mRNAs and differentially hydroxymethylation peaks between two placental shares in sIUGR group and normal MCDA group shown on the heatmap. (c) The differentially expressed mRNAs between larger and smaller placental shares of sIUGR plotted in the volcano plot. One hundred eighty-one upregulated genes and 614 downregulated genes identified in smaller placental shares of the sIUGR group. (d) Expression of hydroxymethylation-regulated associated genes detected in the smaller placental shares compared to the larger ones in sIUGR twin pairs by quantitative RT-PCR.

L, larger foetus; S, smaller foetus. (**$p < 0.01$)

(GO) term from hMeDIP-chip data and mRNA-seq data were used to determine possible hydroxymethylation-associated genes (Figure S3, supplement Table S2).

Fifteen differentially hydroxymethylation-associated genes were found, including 13 upregulated mRNAs associated with high 5 hmC enrichment and 2 downregulated mRNAs associated with low 5 hmC enrichment (Figure 1(a)). Furthermore, Reverse transcription-qPCR(RT-qPCR) was performed to validate the expression of these genes in each of the placental shares from the sIUGR group and the normal group. Among these genes, *ANGPTL4* expression was significantly reduced in smaller placental shares of the sIUGR group (Figure 1(d)). No

significant difference in *ANGPTL4* expression was identified between the two placental shares of the normal group (supplement figure S2).

Hydroxymethylation-associated *ANGPTL4* is decreased in smaller placental shares of sIUGR

RT-qPCR and western blotting were used to further verify the expression of *ANGPTL4* in the placentas of sIUGR and the normal group. The results showed that the mRNA and protein expression levels of *ANGPTL4* were both decreased in the smaller placental shares compared to the larger ones in the sIUGR group, but no differences were observed between the two placental shares of the normal group (Figure 2(a,b)).
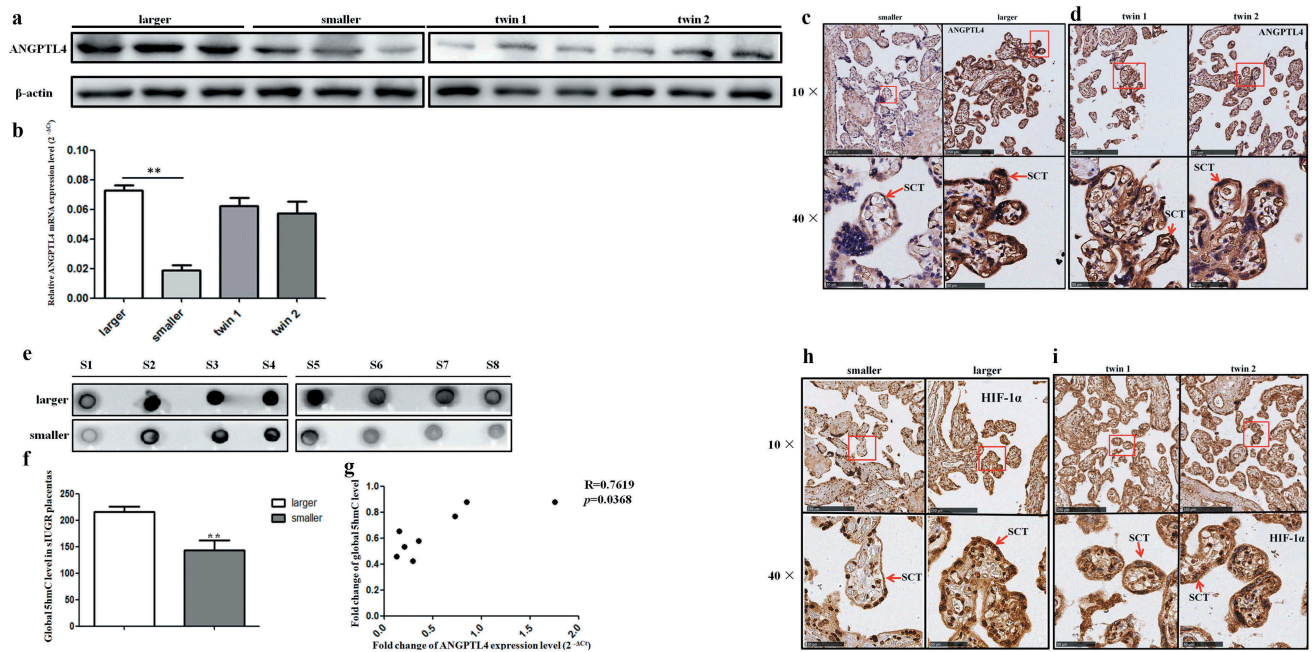
Figure 2. Hydromxymethylation-associated *ANGPTL4* identified in sIUGR twin pairs. (a, b) Decreased *ANGPTL4* detected in smaller placental shares of the sIUGR group compared to the normal MCDA group by western blotting and quantitative RT-PCR. (**$p < 0.01$). (c, d) Single staining of maternal villi from sIUGR (smaller & larger) and normal MCDA group (twin1 & twin2) using *ANGPTL4* antibody was visualized. Above scale bar = 250 μm. Below scale bar = 50 μm. (e, f) Global 5hmC levels detected in two placental shares of sIUGR group by dot blot. S1-8 was eight pairs of sIUGR placentas (smaller & larger). (g) Correlation analysis of *ANGPTL4* expression with global 5hmC level in smaller placental shares compared to larger ones in the sIUGR group. (h, i) Single staining of maternal villi from sIUGR (smaller & larger) and normal MCDA group (twin1 & twin2) using *HIF-1α* antibody was visualized. Above scale bar = 250 μm. Below scale bar = 50 μm. Compared to the normal MCDA group, weaker positive signal for *ANGPTL4* and *HIF-1α* both detected in smaller placental shares than larger ones in the sIUGR group.

Immunohistochemistry (IHC) analysis of placental villous tissues was performed to investigate the localization of *ANGPTL4* in placental villous tissue. A weaker positive signal for *ANGPTL4* was detected in syncytiotrophoblast (SCT) from the smaller placental shares compared to what was observed in the larger ones (Figure 2(c)) in the sIUGR group. In contrast, similar *ANGPTL4* expression was observed in SCT in the two placental shares of the normal group (Figure 2(d)).

In addition, the global 5 hmC level was measured in eight pairs of placental tissues in the sIUGR group by dot blot and was correlated with the level of *ANGPTL4* mRNA expression ($p = 0.037 < 0.05$) (Figure 2(e–g)). These data suggested that decreased *ANGPTL4* expression may be associated with hypohydroxymethylation levels in the smaller placental shares of sIUGR.

We also examined the expression and localization of *HIF-1α* by IHC. As shown in Figure 2(h,i), the signal for HIF-1α was much weaker in SCT from the smaller placental shares than it was in the larger placental shares of the sIUGR group, while no difference was found between two placental shares of the normal group (Figure 2(h,i)).

Reduced ANGPTL4 *suppresses trophoblast invasion and migration*

To address the role of *ANGPTL4* in human trophoblasts, the HTR8/SVneo cell line (HTR8) was transfected with *ANGPTL4* siRNA. RT-qPCR results confirmed that *ANGPTL4* expression was decreased after siRNA transfection, and siRNA3 was the most effective siRNA (Figure 3(a)). Subsequently, *ANGPTL4* siRNA3 was used directly to reduce *ANGPTL4* expression in HTR8 cells.

Liu et al have reported that silenced *ANGPTL4* weakened trophoblast cells migration and invasion [16]. Consistent with Liu et al results, our data showed that reduced *ANGPTL4* drastically inhibited the invasive and migration abilities of HTR8 cells when compared with blank and negative control-siRNA (NC) cells (Figure 3(b–e)). However, HTR8 cells transfected
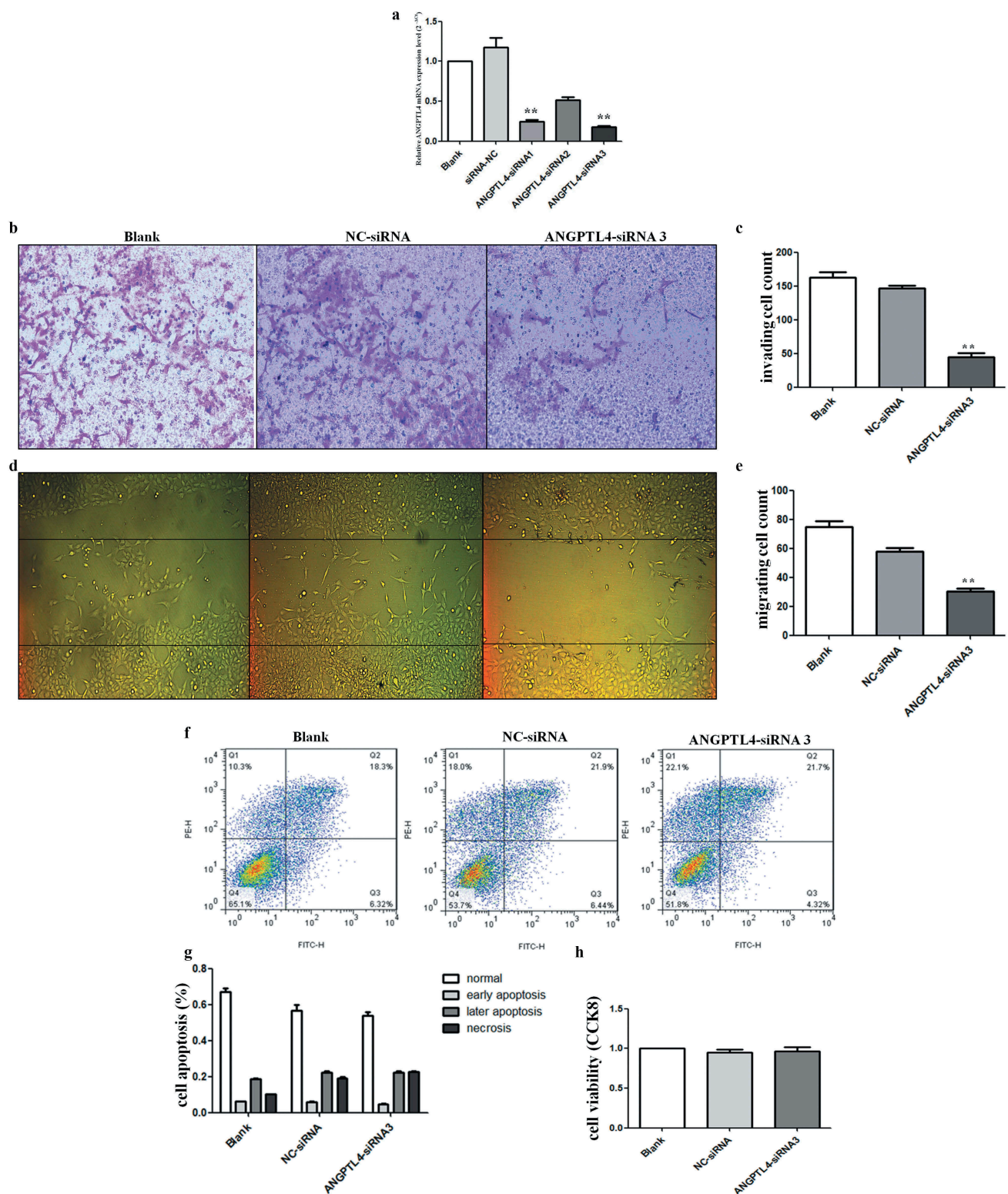
Figure 3. Decreased *ANGPTL4* directly inhibited trophoblast invasion and migration *in vitro*. (a) The expression of *ANGPTL4* when using *ANGPTL4* siRNA. Decreased *ANGPTL4* expression detected when using three siRNAs, of which siRNA3 was the most effective. (b, c) Transwell assays showed that invaded cells reduced when using siRNA3. (**$p < 0.01$). (d, e) Wound healing assays shown that migrated cells decreased when using siRNA3. (**$p < 0.01$). (f, g) No significant difference in the apoptopsis and necrosis detected when using siRNA3 by Flow cytometry (FCM). (h) No significant difference in cell viability identified when using siRNA3 by CCK8 assay.

with the siRNA exhibited no significant changes in cell viability and apoptosis (Figure 3(f–h)). These results indicated that decreased *ANGPTL4* expression suppressed trophoblast invasiveness and migration.

ANGPTL4 is the downstream target of HIF-1α *and is regulated by the HIF-1 signalling pathway*

Previous data have suggested that a hypoxic environment might be related to placental dysfunction. *HIF-1α*, as a hypoxia-induced factor, is also an upstream regulator of *ANGPTL4*. Moreover, IHC data revealed that the localization and expression of *HIF-1α* was positively correlated with *ANGPTL4* (Figure 2(c,d,h,i)). We next investigated the regulatory relationship between *HIF-1α* and *ANGPTL4*, and we determined the underlying mechanisms causing decreased *ANGPTL4* to effect trophoblast functions by using a *HIF-1* agonist (DMOG), a *HIF-1* inhibitor (digoxin), and a *HIF-1α* siRNA.

Western blot results showed that *HIF-1α* and *ANGPTL4* were both highly expressed when using DMOG, and they exhibited low expression levels when using digoxin regardless of normoxic or hypoxic conditions (Figure 4(a–d)). In addition, *HIF-1α* and *ANGPTL4* were also decreased when using *HIF-1α* siRNA compared with blank or NC-siRNA (Figure 4(e,f)).

We next explored the effects of the aberrant *HIF-1* signalling pathway on trophoblast functions. The results revealed that migration and invasive abilities were both enhanced by DMOG, whereas the migration and invasive capacities were weakened (Figure 4 (g–j)) by digoxin. Moreover, late apoptosis and necrosis ratios in trophoblasts were significantly increased when using digoxin compared to the ratios of blank trophoblasts (Figure 4(k,l)). Taken together, *ANGPTL4* expression may be regulated by the *HIF-1* signalling pathway in normoxic or hypoxic conditions. Aberrant *HIF-1* signalling pathway-affected trophoblast functions may target *ANGPTL4*.

Hypoxia leads to aberrant expression of ANGPTL4 *and* HIF-1α*, positively correlated with their aberrant hydroxymethylation levels in promoter regions*

The above results have demonstrated that aberrant *HIF-1α*-regulated *ANGPTL4* may affect trophoblast functions. We next constructed a hypoxic trophoblastic model *in vitro* and further explored the relationship between the expression of *ANGPTL4* and *HIF-1α* and their 5hmC levels in promoter regions by hMeDIP-qPCR and western blotting.

Compared to the normoxic conditions (21% O_2), the expression levels of *ANGPTL4* and *HIF-1α* were both upregulated in 10% O_2-48 hr and downregulated in 1% O_2-48 hr ($p < 0.05$) (Figure 5(a,b)). Meanwhile, the 5 hmC levels of *ANGPTL4* and *HIF-1α* were also increased in 10% O_2-48 hr and decreased in 1% O_2-48 hr ($p < 0.05$) (Figure 5(c,d)). These data suggested that the 5 hmC levels of *ANGPTL4* and *HIF-1α* were positively correlated with their expression in 10% O_2-48 hr and 1% O_2-48 hr; aberrant *ANGPTL4* and *HIF-1α* expression may be related to their aberrant 5 hmC levels of promoter regions in hypoxic conditions.

Discussion

In MC twins with sIUGR, vascular anastomoses and unequal placental territories are thought to be the important reasons for discordant foetal growth and different clinical outcomes [17]. The presence of placental anastomoses and discordant placental shares between two foetuses may interfere with the natural progression of the smaller foetus, leading to the failure to achieve its growth potential. However, the underlying molecular mechanism of sIUGR remains poorly understood. Because almost all MC twins were monozygotic twins, both foetuses of a twin pair harboured identical genomic DNA and grew in a similar intrauterine environment [18]. It is a good model for evaluating the epigenetic-modified mechanism in foetal development and placental dysfunction.

DNA hydroxymethylation is reported to be an important epigenetic modification in different mammalian cells that contributes to the regulation of genomic structure and function [19,20]. In singleton pregnancy, altered 5 hmC levels have been observed in women who are obese, have PE or have gestational diabetes mellitus (GDM) [21–23]. Cardenas et al [24] reported that prenatal mercury exposure was related to decreased 5 hmC levels in cord blood. These results demonstrated that maternal complications or adverse intrauterine environments may influence 5 hmC levels during foetal development.
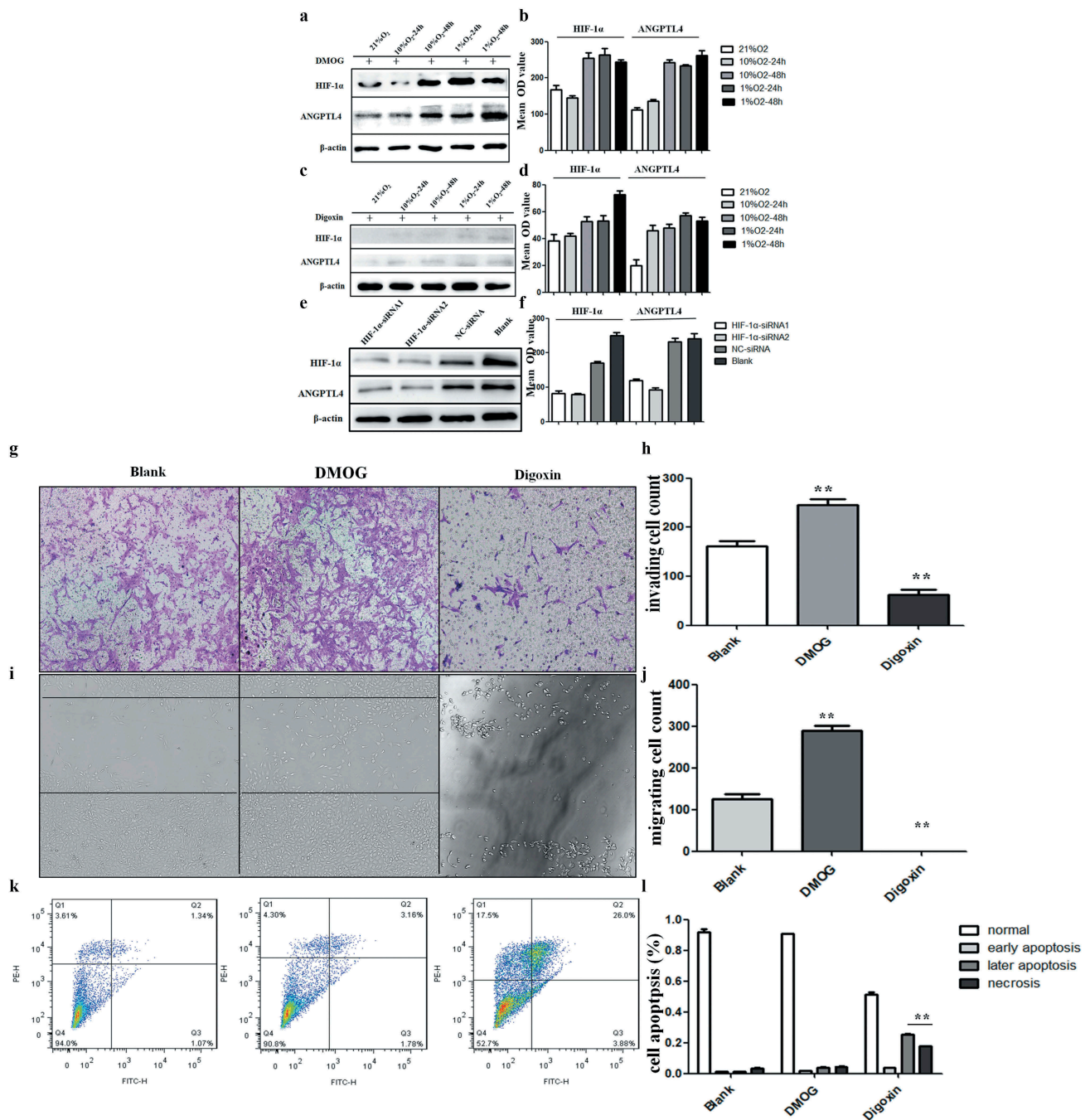
Figure 4. *ANGPTL4* is a downstream target of *HIF-1α* and regulated by *HIF-1* signalling pathway *in vitro*. (a–f) Western blot analysis of *HIF-1α* and *ANGPTL4* expression in HTR8 cells with *HIF-1* agonist (DMOG), *HIF-1* inhibitor (digoxin) and *HIF-1α* siRNA for 48 hours. Expressions of *HIF-1α* and *ANGPTL4* both increased when using DMOG, while decreased by using digoxin or *HIF-1α* siRNA. (g, h) Transwell assays showed that invaded cells increased in DMOG group, and reduced in digoxin group. (**$p < 0.01$). (i, j) Wound healing assays shown that migrated cells increased in DMOG group, and reduced in digoxin group. (**$p < 0.01$). (k, l) FCM results showed that late apoptopsis and necrosis of HTR8 cells increased significantly when using digoxin. (**$p < 0.01$).

In our study, decreased global 5 hmC levels were identified in smaller placental shares compared to larger ones in cases of sIUGR. Furthermore, a possible hydroxymethylation-associated gene, *ANGPTL4*, was identified and verified in sIUGR placentas and hypoxic trophoblasts *in vitro*. This finding suggests that reduced 5 hmC levels and 5 hmC-associated *ANGPTL4* may be related to discordant foetal development and placental dysplasia.

The placenta is a mediator of communication between foetal development and maternal environment. The placenta regulates maternal-foetal
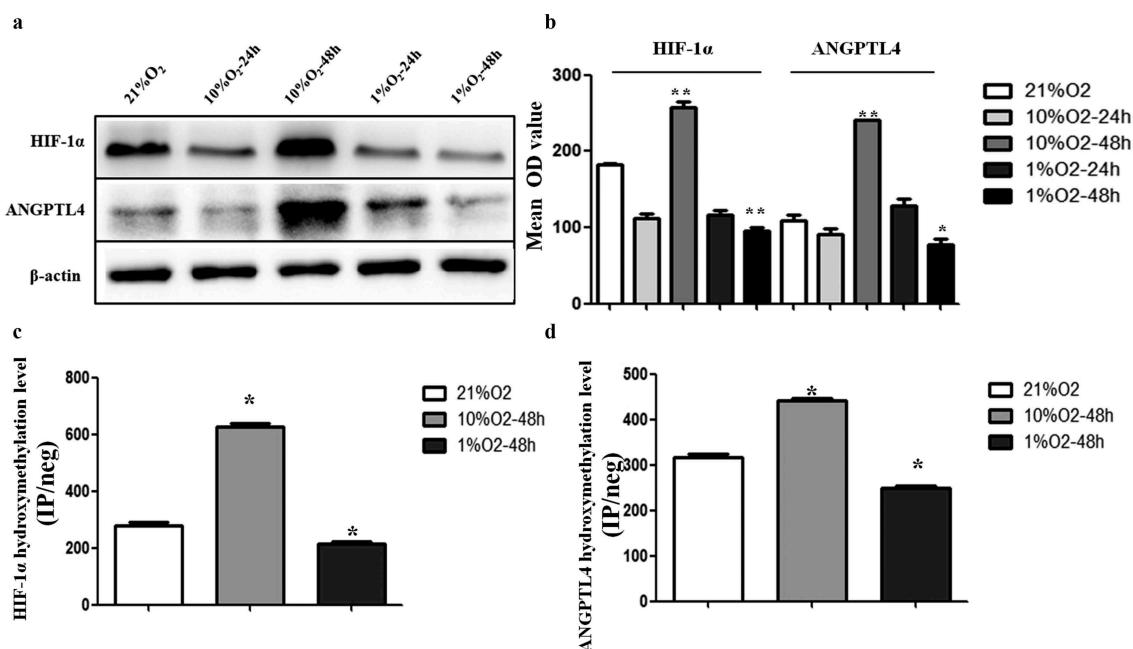
Figure 5. Hypoxia leads to aberrant expression of *ANGPTL4* and *HIF-1α*, positively correlated with their aberrant hydroxymethylation levels in promoter regions. (a, b) Western blot results showed the protein levels of *HIF-1α* and *ANGPTL4* under normoxic conditions with 21%O_2 and under hypoxic conditions with 10% and 1% O_2 for 24 hours and 48 hours. Expression of *HIF-1α* and *ANGPTL4* both highly expressed in 10%O_2-48 hours and reduced expressed in 1%O_2-48 hours. (c, d) The 5hmC levels in the promoters of *HIF-1α* and *ANGPTL4* under normoxic and hypoxic conditions were detected by hMeDIP-qPCR. The percentage of the input is shown as indicated. The results showed that the 5hmC enrichment of *HIF-1α* and *ANGPTL4* increased in 10%O_2-48 hours and reduced in 1%O_2-48 hours. (*$p < 0.05$, **$p < 0.01$).

nutrient and waste exchange, facilitates interactions with the maternal immune system, and acts as a neuroendocrine organ for developing foetuses [25]. Trophoblasts are the main component of the placenta, dysfunction of which will lead to placental dysplasia. In singleton pregnancy, *ANGPTL4* repression regulated by *PVT1* may play an essential role in PE by affecting trophoblast functions [26]. *ANGPTL4* may also be involved in fatty acid-induced angiogenesis *in vitro* [27]. However, a discrepancy among different studies was found, in that *ANGPTL4* has been reported to have a role in angiogenesis, anti-angiogenesis or even pathological angiogenesis [28–30]. In our data, reduced *ANGPTL4* significantly inhibited the invasiveness and migration of trophoblasts, whereas no effect was found in cell viability and apoptosis.

Different environmental factors, which have the potential to alter placental epigenomic profiles, might contribute to placental dysplasia [31]. Environmental oxygen is a potent driver of vascular development in the maternal-foetal interface [32]. Insufficient adaptive responses to too much or too little oxygen may lead to cellular

injury [33]. *HIF-1α* is an important hypoxia-induced factor, and it was confirmed to regulate proliferation, apoptosis and tolerance to hypoxia [34]. Previous studies have reported that *HIF-1α* was associated with the pathology of PE and FGR [35,36]. Hypoxia-induced *HIF-1α* promoted the invasion of trophoblast cells *in vitro* [37]. *ANGPTL4*, as a downstream target of *HIF-1α*, has been verified to be regulated by *HIF-1α* in osteosarcoma cells [14]. Our data showed that the expression and localization of *ANGPTL4* were positively related to *HIF-1α* in the smaller placental shares of sIUGR. In addition, *HIF-1α* knockdown can directly downregulate the expression of *HIF-1α* and *ANGPTL4 in vitro*. The expression of *HIF-1α* and *ANGPTL4* and trophoblast functions were both affected when using a *HIF-1* agonist and inhibitor. Therefore, multiple lines of evidence support the role of *HIF-1α* in affecting trophoblast functions via regulating *ANGPTL4* expression. Interestingly, treatment with an *HIF-1* inhibitor induced trophoblast apoptosis and necrosis, which was not observed following *ANGPTL4* knockdown. It is possible that *HIF-1α*

affects different cell functions via different downstream targets. In fact, *HIF-1α* induces more than 100 target genes to adapt to hypoxic conditions by different regulatory mechanisms [38].

Furthermore, we verified the possible correlation between 5hmC enrichment and the expression changes of *ANGPTL4* and *HIF-1α* under different hypoxic conditions. Previous studies have confirmed positive relationships between the levels of 5 hmC and gene expression in the brain, chondrocytes and embryonic stem cells [39–41]. Consistent with previous data, our results show that 5 hmC levels and expression of *HIF-1α/ANGPTL4* were both increased in 10% O_2 48 hr and decreased in 1% O_2 48 hr, which means that the 5 hmC levels in promoter regions were positively related to gene expression in different oxygen concentrations. These results suggest that hypoxia-induced aberrant expression of *ANGPTL4* and *HIF-1α* may be related to their aberrant 5 hmC levels in promoter regions, which contribute to trophoblast dysfunction and placental dysplasia and further result in disrupted foetal development.

There is a limitation in this study in that we have only one single time point in every placental sample, which is the time for delivery in gestational weeks. In fact, the placental expression profiles and the dynamic regulation of cytosine are known to vary at different trimesters [25]. This suggests that the relationship between 5 hmC and gene expression may be complicated and unique in different gestational weeks.

In summary, this study first demonstrated that the global 5hmC level was decreased in smaller placental shares compared to larger ones in cases of sIUGR. Reduced hydroxymethylation-associated *ANGPTL4* was validated in placentas and trophoblasts *in vitro*. Hypoxia-induced aberrant expression of *ANGPTL4* and *HIF-1α* may be related to their aberrant 5hmC levels in promoter regions, which contribute to trophoblast dysfunction. Therefore, our findings revealed that aberrant hydroxymethylation-associated *ANGPTL4* may be involved in the pathogenesis of sIUGR and may further provide a new epigenetic mechanism in which discordant DNA hydroxymethylation may be associated with phenotypic discrepancies between monozygotic twin foetuses.

Materials and methods

Patients and placental sample collection

From December 2015 to December 2017, a total of 31 MCDA twin pregnancies were enrolled, including 13 pairs of sIUGR twins (sIUGR group) and 18 pairs of normal MCDA twins (normal group). The study was approved by the ethics committee in the hospital. The collection of placental tissues was performed with the patients' informed consent.

The chorionicity was determined by ultrasound at 11–14 weeks as previously described [42], and it was confirmed by placental examination after delivery [43]. sIUGR was defined when the birth weight of one foetus was below the 10th percentile, and the intertwin discordance was greater than 25% [44]. The normal group included normal MCDA twin pregnancies without sIUGR or other complications. Pregnancies with severe maternal complications, twin to twin transfusion syndrome (TTTS), twin-anaemia polycythaemia sequence (TAPS), structural defects and foetal death were excluded.

In sIUGR twin pregnancies, smaller placental shares were the placental sections excised at the region of the umbilical cord insertion point from the restricted foetus (<10th percentile), while larger placental shares were the placental sections of the co-twins.

Placental tissue pieces of approximately 2 × 2 × 1 cm^3 were excised immediately after delivery by caesarean section from placentas at the region around the individual umbilical cord insertion point, rinsed with ice-cold phosphate-buffered saline (PBS) and stored appropriately for subsequent experiments.

Cell culture, reagents and transfection

HTR8/SVneo (HTR8) was obtained from American Type Culture Collection (ATCC). Hypoxia was induced in a hypoxic incubator with 1% or 10% O_2 for 24 and 48 hr. DMOG (Catalogue No. A4506), a *HIF-1* agonist, and digoxin (Catalogue No. B7684), a *HIF-1* inhibitor, were purchased from APExBIO. DMOG and digoxin were both diluted at a concentration of 10 μmol/L and cultured with HTR8 cells for 24 and 48 hr. *ANGPTL4* and *HIF-1α* knockdown was achieved using small

interfering RNA (siRNAs; Gene Pharma) introduced via Lipofectamine 3000 (Invitrogen, Catalogue No. L3000015) according to the manufacturer's instructions. The sequences of the oligonucleotides are listed in supplement Table S3.

hMeDIP-Chip and data processing

Four pairs of sIUGR placentas and four pairs of normal MCDA placentas were used in hMeDIP-Chip. Genomic DNA was extracted from placentas by a DNeasy Blood and Tissue Kit (Qiagen, Catalogue No. 69506) and sonicated to fragments of 200–1000 bp with a Bioruptor sonicator (Diagenode).

Differential enrichment peaks (DEP) were calculated by M' value as follows: $M' = \text{Average} (\log_2 \text{hMeDIP}^{\text{smaller foetus}}/\text{Input}^{\text{smaller foetus}}) - \text{Average} (\log_2 \text{hMeDIP}^{\text{larger foetus}}/\text{Input}^{\text{larger foetus}})$. Gene ontology (GO) terms and Kyoto Encyclopaedia of Genes and Genomes (KEGG) pathways were also analysed via their online databases (http://www.geneontology.org/, http://www.kegg.jp/, respectively) [45].

mRNA sequencing

Four pairs of sIUGR placentas and four pairs of normal MCDA placentas were used in mRNA sequencing. Total mRNA from placentas was isolated by using a KAPA Stranded RNA-Seq Library Preparation Kit (Illumina platforms) (KAPA Biosystems, Catalogue No. KK8401). The completed libraries were qualified on an Agilent 2100 Bioanalyzer, quantified and sequenced on an Illumina HiSeq 4000 (Illumina) according to the manufacturer's instructions.

After sequencing, base calling was carried out using Off-Line Base caller software (version V1.8.0; Illumina). The trimmed reads that passed sequence quality examination and trimmed 5′,3′-adaptor bases using cutadapt [46], were aligned to the reference genome by HISAT 2 software (v2.0.4) [47]. StringTie (v1.2.3) [48] and R package Ballgown (v2.6.0) [49] were used to calculate the transcript abundance and the FPKM value [50] for gene and transcript levels. The differentially expressed genes and transcripts were filtered by using the R package Ballgown.

RNA extraction and reverse transcription-qPCR validation

Thirteen pairs of placental samples from sIUGR twins and eighteen pairs of placental samples from normal MCDA twins were used to perform RT-qPCR to detect the mRNA expression of candidate genes. Total RNA was extracted using RNAiso Plus (Takara, Catalogue No. 9109) according to the manufacturer's protocol. cDNA was synthesized from total RNA using PrimeScript RT Master Mix (TaKaRa, Catalogue No. RR036A), and then, real-time PCR was performed with SYBR Premix Ex Taq II (Takara, Catalogue No. RR820A) on an ABI 7500 Real-Time PCR System (Thermo Fisher Scientific) using the $2^{-\Delta\Delta Ct}$ method. A list of primers is available in supplement Table S4.

Western blot, dot blot and immunohistochemistry

Thirteen pairs of sIUGR placentas and eighteen pairs of normal MCDA placentas were used to perform western blotting to detect the protein expression of ANGPTL4 and HIF-1α according to the standard protocol [51]. Eight pairs of sIUGR placentas and eight pairs of normal MCDA placentas were used in immunohistochemistry (IHC). Meanwhile, eight pairs of sIUGR placentas were also used in dot blot to detect the global 5hmC level in sIUGR group. Genomic DNA was extracted from placental tissues by a MiniBEST FFPE DNA Extraction Kit (TaKaRa, Catalogue No. 9782), and the concentrations were measured using a NanoDrop™ 2000 Spectrophotometer (Thermo Scientific). Primary antibodies against ANGPTL4 (1:250) (Abcam, Catalogue No. ab196746), HIF-1α (1:200) (Abcam, Catalogue No. ab82832) and 5hmC (1:500) (Abcam, Catalogue No. ab214728) were used and were then visualized by Immobilon™ Western chemiluminescent HRP substrate (Millipore, Catalogue No. WBKLS0500). Quantification of images was performed using

ImageJ software. Staining for IHC was visualized by DAB (Beyotime, Catalogue No. P0203). High-resolution digital images were acquired with a NanoZoomer S360 Slide Scanner (Hamamatsu) and were then analysed by NDP.view2 Viewing software (Hamamatsu).

hMeDIP-qPCR

A hMeDIP assay combined with qPCR was used to quantitatively evaluate the hydroxymethylation status of *ANGPTL4* and *HIF-1α* in normoxic and hypoxic trophoblasts. hMeDIP was performed according to a previously published method [52]. The primer sequences are listed in supplement Table S5. This experiment was performed in triplicate. The relative changes in the extent of promoter hydroxymethylation were determined by calculating the amount of promoter in immunoprecipitated DNA after normalization to the input DNA: %(hMeDNA-IP/Input) = 2 $(Ct^{input}-Ct^{hMeDNA-IP})$ ×Input dilution factor×100%.

Cell migration analysis

Migration analysis was performed with the wound healing assay to investigate the trophoblast migration ability *in vitro*. Cells were seeded and treated the next day with *ANGPTL4* siRNA, DMOG and digoxin. Subsequently, a wound was made in each well with the use of a sterile micropipette tip, and cells were cultured for an additional 48 hours. Photographs were taken and used for analysis by ImageJ software.

Cell invasion assay

A transwell invasion assay was used to investigate trophoblast invasion ability *in vitro*. A 24-transwell plate (Co-Star) was coated with 100 μl of BD Matrigel (BD Biosciences, Catalogue No. 356234). Cells were suspended in FBS-free medium, and 100 μl were transferred into the upper chamber of the transwell. The lower chamber was filled with 600 μl of medium containing 10% FBS. After incubation for 48 hours, the Matrigel was removed with a cotton swab, and invaded cells were stained with crystal violet.

Cell viability analysis

CCK8 assays were used to detect trophoblast viability (Beyotime, Catalogue No. C0038). Cells were placed in 96-well plates and treated with *ANGPTL4* siRNA, DMOG or digoxin. Then, the cells were cultured with 10 μl of CCK8 reagent in the incubator for 2 hours at 37°C. Cell viability was measured by a microplate reader at a wavelength of 450 nm.

Cell apoptotic ratio assay

Cell apoptosis assays were performed by an Annexin V-FITC Cell Apoptosis kit (Beyotime, Catalogue No. C1062 L) to detect trophoblast apoptosis and necrosis ratio according to the manual instructions. In brief, cells were treated with *ANGPTL4* siRNA, DMOG or digoxin, washed with PBS twice, washed with 1× binding buffer once and then suspended in 1× binding buffer. Cells were double-stained with Annexin V-FITC and PI for 15 minutes in the dark at room temperature and then analysed by flow cytometry (BD).

Statistical analysis

All statistical values were calculated using SPSS 22.0 (Chicago, IL, USA) and GraphPad Prism 5. Experimental groups were analysed by independent sample t-tests when comparing between 2 groups and one-way ANOVA when comparing among multiple groups. Correlations were analysed using Spearman's rank correlation test. Data are presented as the mean ± SD. All *p* values are two-sided. A *p* value of < 0.05 was considered to indicate statistical significance.

ORCID

Yi Zhang ⬤ http://orcid.org/0000-0002-7936-8777

References

[1] Rustico MA, Consonni D, Lanna M, et al. Selective intrauterine growth restriction in monochorionic twins: changing patterns in umbilical artery Doppler flow and outcomes. Ultrasound Obstet Gynecol. 2017;49(3):387–393.

[2] He Z, Lu H, Luo H, et al. The promoter methylomes of monochorionic twin placentas reveal intrauterine growth restriction-specific variations in the methylation patterns. Sci Rep. 2016;6:20181.

[3] Wen H, Chen L, He J, et al. MicroRNA expression profiles and networks in placentas complicated with selective intrauterine growth restriction. Mol Med Rep. 2017;16(5):6650–6673.

[4] Shukla A, Sehgal M, Singh TR. Hydroxymethylation and its potential implication in DNA repair system: A review and future perspectives. Gene. 2015;564(2):109–118.

[5] Zhao J, Ma XL, Ma JX, et al. TET3 mediates alterations in the epigenetic marker 5hmC and Akt pathway in steroid-associated osteonecrosis. J Bone Miner Res. 2017;32(2):319–332.

[6] Fischer AP, Miles SL. Silencing HIF-1α induces TET2 expression and augments ascorbic acid induced 5-hydroxymethylation of DNA in human metastatic melanoma cells. Biochem Biophys Res Commun. 2017;490(2):176–181.

[7] Hsieh TH, Liu YR, Chang TY, et al. Global DNA methylation analysis reveals miR-214-3p contributes to cisplatin resistance in pediatric intracranial nongerminomatous malignant germ cell tumors. Neuro Oncol. 2018;20(4):519–530.

[8] Shi DQ, Ali I, Tang J, et al. New insights into 5hmC DNA modification: generation, distribution and function. Front Genet. 2017;8:100.

[9] Chen X, Chen K, Feng Y, et al. The potential role of pregnancy-associated plasma protein-A2 in angiogenesis and development of preeclampsia. Hypertens Res. 2019;42(7):970–980.

[10] Gunatillake T, Chui A, Fitzpatrick E, et al. Decreased placental glypican expression is associated with human fetal growth restriction. Placenta. 2019;76:6–9.

[11] Li L, Huang X, He Z, et al. miRNA-210-3p regulates trophoblast proliferation and invasiveness through fibroblast growth factor 1 in selective intrauterine growth restriction. J Cell Mol Med. 2019;23(6):4422–4433.

[12] Luo YM, Fang Q, Shi HJ, et al. Imprinting and promoter usage of insulin-like growth factor II in twin discordant placenta. Obstet Gynecol Int. 2010;2010:498574.

[13] Yang X, Cheng Y, Su G. A review of the multifunctionality of angiopoietin-like 4 in eye disease. Biosci Rep. 2018;38(5):BSR20180557.

[14] Zhang T, Kastrenopoulou A, Larrouture Q, et al. Angiopoietin-like 4 promotes osteosarcoma cell proliferation and migration and stimulates osteoclastogenesis. BMC Cancer. 2018;18(1):536.

[15] Huang CZ, Xu JH, Zhong W, et al. Sox9 transcriptionally regulates Wnt signaling in intestinal epithelial stem cells in hypomethylated crypts in the diabetic state. Stem Cell Res Ther. 2017;8(1):60.

[16] Liu L, Zhuang X, Jiang M, et al. ANGPTL4 mediates the protective role of PPARγ activators in the pathogenesis of preeclampsia. Cell Death Dis. 2017;8(9):e3054.

[17] Bennasar M, Eixarch E, Martinez JM, et al. Selective intrauterine growth restriction in monochorionic diamniotic twin pregnancies. Semin Fetal Neonatal Med. 2017;22(6):376–382.

[18] Xiang Z, Yang Y, Chang C, et al. The epigenetic mechanism for discordance of autoimmunity in monozygotic twins. J Autoimmun. 2017;83:43–50.

[19] Etchegaray JP, Chavez L, Huang Y, et al. The histone deacetylase SIRT6 controls embryonic stem cell fate via TET-mediated production of 5-hydroxymethylcytosine. Nat Cell Biol. 2015;17(5):545–557.

[20] Spiers H, Hannon E, Schalkwyk LC, et al. 5-hydroxymethylcytosine is highly dynamic across human fetal brain development. BMC Genomics. 2017;18(1):738.

[21] Mitsuya K, Parker AN, Liu L, et al. Alterations in the placental methylome with maternal obesity and evidence for metabolic regulation. PLoS One. 2017;12(10):e186115.

[22] Ma M, Zhou QJ, Xiong Y, et al. Preeclampsia is associated with hypermethylation of IGF-1 promoter mediated by DNMT1. Am J Transl Res. 2018;10(1):16–39.

[23] Sun M, Song MM, Wei B, et al. 5-Hydroxymethylcytosine-mediated alteration of transposon activity associated with the exposure to adverse in utero environments in human. Hum Mol Genet. 2016;25(11):2208–2219.

[24] Cardenas A, Rifas-Shiman SL, Godderis L, et al. Prenatal exposure to mercury: associations with global DNA methylation and hydroxymethylation in cord blood and in childhood. Environ Health Perspect. 2017;125(8):87022.

[25] Green BB, Houseman EA, Johnson KC, et al. Hydroxymethylation is uniquely distributed within term placenta, and is associated with gene expression. Faseb J. 2016;30(8):2874–2884.

[26] Xu Y, Lian Y, Zhang Y, et al. The long non-coding RNA PVT1 represses ANGPTL4 transcription through binding with EZH2 in trophoblast cell. J Cell Mol Med. 2018;22(2):1272–1282.

[27] Basak S, Duttaroy AK. Effects of fatty acids on angiogenic activity in the placental extravillious trophoblast cells. Prostaglandins Leukot Essent Fatty Acids. 2013;88(2):155–162.

[28] Chomel C, Cazes A, Faye C, et al. Interaction of the coiled-coil domain with glycosaminoglycans protects angiopoietin-like 4 from proteolysis and regulates its antiangiogenic activity. Faseb J. 2009;23(3):940–949.

[29] Hu K, Babapoor-Farrokhran S, Rodrigues M, et al. Hypoxia-inducible factor 1 upregulation of both VEGF and ANGPTL4 is required to promote the angiogenic phenotype in uveal melanoma. Oncotarget. 2016;7(7):7816–7828.

[30] Babapoor-Farrokhran S, Jee K, Puchner B, et al. Angiopoietin-like 4 is a potent angiogenic factor and a novel therapeutic target for patients with proliferative diabetic retinopathy. Proc Natl Acad Sci U S A. 2015;112(23):E3030–E3039.

[31] Lee SA, Ding C. The dysfunctional placenta epigenome: causes and consequences. Epigenomics. 2012;4(5):561–569.

[32] Falkowski PG, Katz ME, Milligan AJ, et al. The rise of oxygen over the past 205 million years and the evolution of large placental mammals. Science. 2005;309(5744):2202–2204.

[33] Samanta D, Prabhakar NR, Semenza GL. Systems biology of oxygen homeostasis. Wiley Interdiscip Rev Syst Biol Med. 2017;9(4):e1382.

[34] Ge L, Wang Y, Cao Y, et al. MiR-429 improved the hypoxia tolerance of human amniotic cells by targeting HIF-1alpha. Biotechnol Lett. 2018;40(11–12):1477–1486.

[35] Verma S, Pillay P, Naicker T, et al. Placental hypoxia inducible factor −1alpha & CHOP immuno-histo-chemical expression relative to maternal circulatory syncytiotrophoblast micro-vesicles in preeclamptic and normotensive pregnancies. Eur J Obstet Gynecol Reprod Biol. 2018;220:18–24.

[36] Robb KP, Cotechini T, Allaire C, et al. Inflammation-induced fetal growth restriction in rats is associated with increased placental HIF-1alpha accumulation. PLoS One. 2017;12(4):e175805.

[37] Highet AR, Khoda SM, Buckberry S, et al. Hypoxia induced HIF-1/HIF-2 activity alters trophoblast transcriptional regulation and promotes invasion. Eur J Cell Biol. 2015;94(12):589–602.

[38] Oh ET, Kim CW, Kim SJ, et al. Docetaxel induced-JNK2/PHD1 signaling pathway increases degradation of HIF-1alpha and causes cancer cell death under hypoxia. Sci Rep. 2016;6:27382.

[39] Kroeze LI, van der Reijden BA, Jansen JH. 5-Hydroxymethylcytosine: an epigenetic mark frequently deregulated in cancer. Biochim Biophys Acta. 2015;1855(2):144–154.

[40] Wen L, Li X, Yan L, et al. Whole-genome analysis of 5-hydroxymethylcytosine and 5-methylcytosine at base resolution in the human brain. Genome Biol. 2014;15(3):R49.

[41] Taylor SE, Li YH, Wong WH, et al. Genome-wide mapping of DNA hydroxymethylation in osteoarthritic chondrocytes. Arthritis Rheumatol. 2015;67(8):2129–2140.

[42] Sepulveda W, Sebire NJ, Hughes K, et al. The lambda sign at 10-14 weeks of gestation as a predictor of chorionicity in twin pregnancies. Ultrasound Obstet Gynecol. 1996;7(6):421–423.

[43] Gao Y, He Z, Wang Z, et al. Increased expression and altered methylation of HERVWE1 in the human placentas of smaller fetuses from monozygotic, dichorionic, discordant twins. PLoS One. 2012;7(3):e33503.

[44] Groene SG, Tollenaar L, Slaghekke F, et al. Placental characteristics in monochorionic twins with selective intrauterine growth restriction in relation to the umbilical artery Doppler classification. Placenta. 2018;71:1–5.

[45] Huang DW, Sherman BT, Lempicki RA. Systematic and integrative analysis of large gene lists using DAVID bioinformatics resources. Nat Protoc. 2009;4(1):44–57.

[46] Chen C, Khaleel SS, Huang H, et al. Software for pre-processing Illumina next-generation sequencing short read sequences. Source Code Biol Med. 2014;9:8.

[47] Kim D, Langmead B, Salzberg SL. HISAT: a fast spliced aligner with low memory requirements. Nat Methods. 2015;12(4):357–360.

[48] Pertea M, Pertea GM, Antonescu CM, et al. StringTie enables improved reconstruction of a transcriptome from RNA-seq reads. Nat Biotechnol. 2015;33(3):290–295.

[49] Frazee AC, Pertea G, Jaffe AE, et al. Ballgown bridges the gap between transcriptome assembly and expression analysis. Nat Biotechnol. 2015;33(3):243–246.

[50] Mortazavi A, Williams BA, McCue K, et al. Mapping and quantifying mammalian transcriptomes by RNA-Seq. Nat Methods. 2008;5(7):621–628.

[51] Li XC, Jin F, Wang BY, et al. The m6A demethylase ALKBH5 controls trophoblast invasion at the maternal-fetal interface by regulating the stability of CYR61 mRNA. Theranostics. 2019;9(13):3853–3865.

[52] Huang N, Tan L, Xue Z, et al. Reduction of DNA hydroxymethylation in the mouse kidney insulted by ischemia reperfusion. Biochem Biophys Res Commun. 2012;422(4):697–702.